

<http://dx.doi.org/10.12785/ijtfst/030308>

Effect of γ -irradiation on Structural and Optical Ellipsometry Parameters of ZnO Nanocrystalline Thin Films

E. R. Shaaban^{1,*}, A. M. A. Mostafa¹, H. Shokry Hassan², M. S. Abd El-Sadek³, Gehan Y. Mohamed³ and I. Sharaf¹

¹ Department of Physics, Faculty of Science, Al-Azhar University, Assiut 71542, Egypt

² Advanced Technology and New Materials Research Institute, City of Scientific Research and Technology Applications, New Borg El-Arab City, Alexandria 21934, Egypt

³ Nanomaterial Laboratory, Physics Department, Faculty of Science, South Valley University, Qena 83523, Egypt

*E-mail: esam_ramadan2008@yahoo.com

Received: 24 Feb. 2014, Revised: 17 Jun. 2014, Accepted: 9 Aug. 2014

Published online: 1 Sep. 2014

Abstract

In the present work, The ZnO powder was prepared by sol-gel method. The microstructure and surface morphology of ZnO powder were characterized by thermo gravimetric (T_G) analysis, differential scanning calorimeter (DSC) and X-ray diffraction (XRD). Thin film of ZnO was prepared using thermal evaporation technique. The effect of γ -irradiation with different doses (100, 300 and 500 kGy) on the structural and optical properties of ZnO thin film were studied. The microstructure parameters, e.g., crystallite size and microstrain for three different doses were calculated. The optical constants (n , k) for three different doses of γ -irradiation of ZnO thin film were obtained by fitting the ellipsometric parameters (ψ and Δ) data using three layer model systems in the wavelength range 300–1100 nm. It is found that the refractive index, n increases with increasing the doses of γ -irradiation. But the obtained optical energy gap of nanocrystalline ZnO films was found to decrease with increasing the doses of the γ -radiation.

Keywords: ZnO nanocrystalline; thin film; γ -irradiation; XRD; Spectroscopic ellipsometry

1- Introduction

Recently, nanocrystalline thin films with a uniform size and shape have shown interesting properties particularly nanocrystalline of metal oxides, due to its numerous important properties such as catalytic,

electrical and optical properties [1, 2].

In materials science, ZnO is often called a II-VI semiconductor because zinc and oxygen belong to the 2nd and 6th groups of the periodic table, respectively. This semiconductor has several favorable properties: good transparency, high electron mobility, wide band gap, strong room temperature luminescence, etc. Those

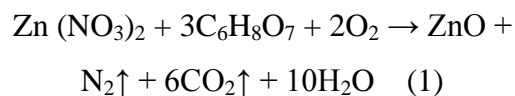
properties are already used in emerging windows, and electronic applications of ZnO as thin-film transistor and light-emitting diode are forth coming as of 2009 [3-6]. Thin films of Zinc oxide can be prepared by various techniques; among them are Sputtering [7], Chemical Vapor Deposition (CVD) [8], Laser ablation [9], Sol-gel [10], Spray pyrolysis [11]. Inoguchi and co-workers [12] have studied structural & optical properties of nanocrystalline ZnO thin films derived from clear emulsion of monodispersed ZnO nanocrystals. Spectroscopic ellipsometry (SE) is a sensitive, precise and non-destructive technique for investigating the optical constants, refractive index, n and extinction coefficient, k of thin films. By measuring the change in the polarization state, i.e., psi (ψ) and delta (Δ), of the light reflected off the surface of a film and subsequently utilizing an appropriate optical/dispersion model, one can extract precisely the optical properties and determine accurately the thickness of the film under study. It is well known that high energy radiation like γ -rays changes the physical properties of thin film materials [13]. The changes occurred are strongly

dependent on the internal structure of the absorbed films, the radiation energy and the amount of doses. The incident radiation may cause ionization or excitation of the electrons revolving in atomic levels. The ability to detect high energy radiation such as X-rays, γ -rays and other uncharged radiation attracts more attention in recent years. This is of great importance in a wide range of applications, including medical imaging, industrial process monitoring, environmental safety and remediation and also in basic science. The present paper has more one fold the first was the preparation of both powder and thin film of ZnO of the hexagonal wurtzite structure. The second was the influence of gamma radiation with different doses on nonstructural the optical parameters of ZnO nanocrystalline thin film. The third was exploiting the spectroscopic ellipsometry for investigating the optical properties of different doses of ZnO films by using three layer model.

2- Experimental

Analytical grade zinc nitrate [$\text{Zn}(\text{NO}_3)_2 \cdot 6\text{H}_2\text{O}$] and citric acid [$\text{C}_6\text{H}_8\text{O}_7 \cdot \text{H}_2\text{O}$] were used to prepare the nano ZnO powder. Metal nitrates

and citric acid were dissolved in deionized water. Nitrate solutions were standardized through chemical analysis using ethylenediamine tetra acetic acid (EDTA) complexometric titration. Nitrate and citric acid solutions were mixed in 1:1 molar ratio of nitrates to citric acid. Then the solution was heated at 80°C to transform into gel. When ignited at any point of the gel, the dried gel burnt in a self-propagating combustion manner until all gels were completely burnt out to form a fluffy loose powder. The experimental observation revealed that the nitrate-citrate gels exhibited self-propagating combustion behavior. Figure 1 shows the DTA and TGA of the dried nitrate-citrate gel. There is one DSC endothermic peak at about 140°C and it may be due to the removal of residual water. This dehydration process is shown 4% weight losses in TGA graph. The DSC exothermic peak at around 186°C may be caused by the autocatalytic anionic oxidation-reduction reaction of nitrates with citric acid, which initiates the formation of nano ZnO powder through the solid-state diffusion process. The nitrate-citrate combustion reaction is as follows:



During combustion CO₂, N₂ and H₂O gasses are released. The thermo gravimetric analysis of the dried gels is exhibited a two-step weight loss. The weight loss at 50-140°C region corresponds to the dehydration of nitrate-citrate gel, while that at 186°C corresponds to the decomposition of nitrate-citrate dried gels as stated in the above reaction. The decomposition at 186°C is shown 17% weight losses in TG graph. This weight loss is attributed to the loss of residual nitrate and organic matters, not the actual nitrate and organic matters as stated in Eq.1. The thermal behavior of the precursor was analyzed by thermogravimetric analysis (TGA) and differential scanning calorimetry (DSC) (Shimadzu 50 with an accuracy of ±0.1 K). The structure and phases of the powder sample was identified by means of X-ray powder diffraction (XRD) Shimadzu Diffractometer XRD 6000, Japan, with Cu-Kα₁ radiation (λ = 1.54056 Å). The data were collected by step-scan modes in a θ -2θ range between 4° and 80° with step-size of 0.02° and step time of 0.6 seconds. Pure Silicon ~ Si 99.9999 % was used

as an internal standard. The deposited film was irradiated with γ -rays obtained from a ^{60}Co source in the Indian γ -chamber mode 14.000/A (available at Atomic Energy Authority, Nassr city, Cairo, Egypt). The average dose rate from the chamber was 1 Gy/s. The SE parameters (ψ and Δ) for ZnO films were measured with a rotating-compensator instrument (J.A. Woollam, M-2000) in the wavelength range 300–1100 nm. The data were acquired at angle of incidence of 70° . All the measurements were conducted at room temperature. The optical constants of the ZnO films before and after irradiated with γ -rays were determined by fitting the model function to the measured data using J.A. Woollam Corporation developed WVASE32 program.

3- Results and discussion

3.1. Thermal analysis and structure characterization with γ -irradiation

Fig. 1 shows thermal curves of the precursor. From the TGA curve, it can be seen that except for the weight loss before 180°C , which is due to loss of physical absorbed water on the surface of the precursor. Most of the weight loss of the precursor takes place between 186°C and 200°C , which is caused by the thermal decomposition

of the precursor; there is no weight loss at T_G curve, indicating that the decomposition is complete. Accordingly, a strong exothermic peak on DSC curve appears between 185°C and 210°C . The purity and crystallinity of the as-synthesized ZnO nanoparticles were examined by using powder X-ray diffraction (XRD) as shown in Fig. 2. It can be seen from Fig. 2 that the diffraction peaks are broad due to the small size of the particle. All these diffraction peaks can be perfectly indexed to the hexagonal Wurtzite of ZnO, not only in peak position, but also in their relative intensity of the characteristic peaks, which is in accordance with that of the standard spectrum (JCPDS, No. 01-1136). The XRD pattern shows that the samples are single phase and no any other impurities distinct diffraction peak except the characteristic peaks of hexagonal Wurtzite phase ZnO was detected.

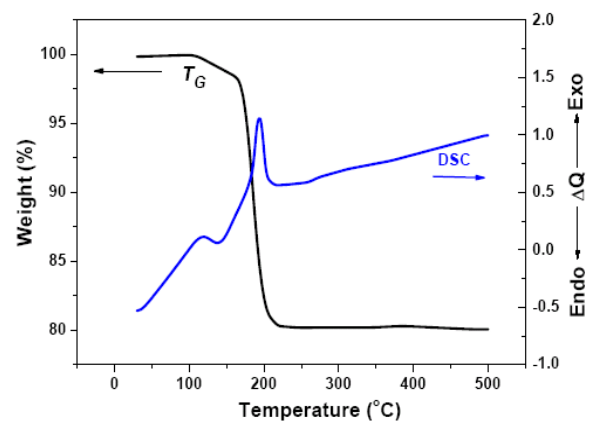


Fig.1: TGA and DSC curves of the precursor.

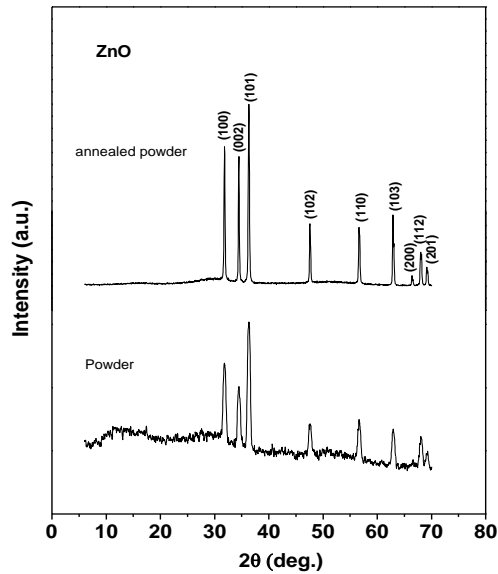


Fig. 2: The XRD patterns of precursor powder and annealed powder of ZnO

Fig. 3 illustrates the X-ray diffraction (XRD) spectra of ZnO thin films of the as deposited and γ -irradiated at exposure doses of 100, 300 and 500 kGy. XRD diffraction peaks belonging to (100), (002), and (101) planes were observed in all as deposited and γ -irradiated of ZnO films. Compared to powder diffraction data of hexagonal Wurtzite structure, the XRD patterns of all the samples indicated enhanced intensities for the peaks corresponding to (002) plane, indicating preferential orientation along the c-axis. The (002)

direction is the close-packing direction of the hexagonal Wurtzite structure and this type of textured growth has often been observed in polycrystalline ZnO films grown on amorphous substrates. Both crystallite size (D_v) and microstrain (e) of the ZnO films were calculated by analyzing the XRD data using the Scherrer's formula, $D_v = k\lambda/\beta\cos(\theta)$ and Wilson formula $e = \beta/(4\tan(\theta))$, respectively; where $\beta = \sqrt{\beta_{\text{obs}}^2 - \beta_{\text{ref}}^2}$ [14]. Both β_{abs} and β_{ref} are the breadth (in radians) of the same Bragg-peak from the XRD scans of the experimental and reference powder, respectively. The reference powder was of ZnO annealed at 300 °C for 2 h. Fig. 4 shows a comparative look of (D_v) and (e) of the ZnO films of different doses of γ -radiation on glass substrate. It is observed that the crystallite size increases but the lattice strain decreases with increasing the doses of γ -radiation. Higher crystallite size results in a lower density of grain boundaries, which behaves as barriers for carrier transport and traps for free carrier. Hence, an increase of crystallite size can cause a decrease of grain boundary scattering. The increasing of the (D_v) maybe owe to the thermal effect during irradiation, which increases the crystallinity of

film. But the decrease in (e) may be attributed to the reduction of lattice imperfections among the grain boundaries, which due to the thermal effect during γ -irradiation.

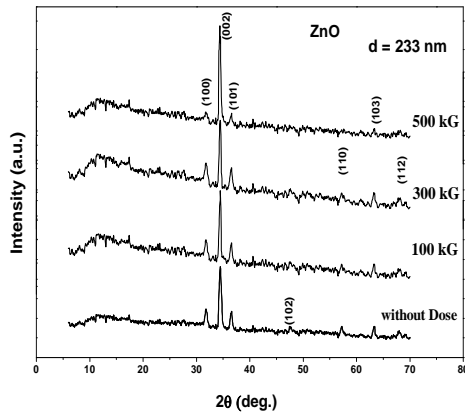


Fig. 3: XRD patterns of the as-deposited and γ -irradiated doses of ZnO films on glass substrates.

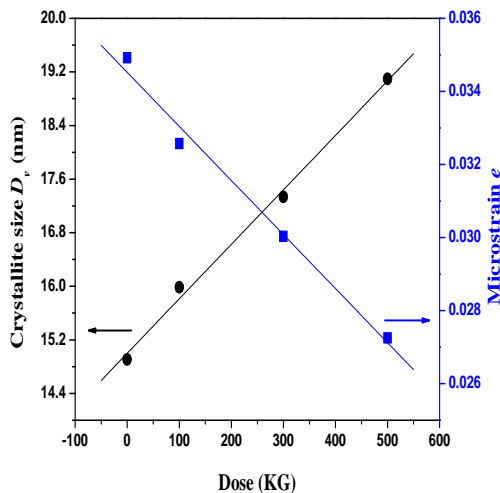


Fig. 4: Effect of γ -irradiated doses of both crystallite size and microstrain of ZnO thin films

3.2. Effect of γ -radiation on optical constants of ZnO in terms of spectroscopic ellipsometry.

The optical properties of for the as deposited and γ -irradiated at exposure doses of 100, 300 and 500 kGy of ZnO films on glass substrate have been studied by spectroscopic ellipsometry (SE), which measures two values ψ and Δ that expresses the amplitude ratio and phase difference between the perpendicular 's' and parallel 'p' polarizations of the reflected light from the sample. The appropriate experimental setups are required which determine non-redundant optical parameters from a general anisotropic sample. Generalized Ellipsometry (GE) comprises theory and experiment of anisotropy in layered samples. The experimental parameters obtained by reference SE (ψ and Δ) are related to the structural and optical properties as defined by [15]:

$$\rho = \frac{r_p}{r_s} = \tan \psi \exp(i \Delta) \quad (2)$$

Here r_s and r_p are the complex Fresnel's reflection coefficients of the light polarized parallel (r_p) and perpendicular (r_s) to the plane of incidence, respectively. The layer model analysis, based on Fresnel's coefficients of reflection, was

performed on the measured ellipsometric angles.

The spectral dependencies of ψ and Δ were fitted in appropriate model to extract the film thickness and optical constants, i.e. refractive index (n) and extinction coefficient (k), using a least square regression analysis and a weighted root mean square error function. The ellipsometric study, by a simple model, which consists of three layers as follows, upper layer (rough layer)/ absorbing ZnO layer/ glass substrate. The upper layer corresponds to the microscopic roughness obtained by SE is well correlated with the mean square error. The program is based on the least square regression to obtain the unknown fitting parameters and their maximum confidence limit. The step is to vary fitting parameters to minimize the difference between the measured and calculated ψ and Δ values. The mean squared error (MSE) could be minimized in terms of Levenberg–Marquardt regression algorithm [16]:

$$MSE = \frac{1}{2N-M} \sum_{i=1}^N \left(\left(\frac{\psi_i^{\text{mod}} - \psi_i^{\text{exp}}}{\sigma_{\psi,i}^{\text{exp}}} \right)^2 + \left(\frac{\Delta_i^{\text{mod}} - \Delta_i^{\text{exp}}}{\sigma_{\Delta,i}^{\text{exp}}} \right)^2 \right) \quad (3)$$

Which has been used to judge the quality of the fit between the measured and the modeled data and is minimized in the fit? Here N is the number of measured ψ and Δ pairs included in the

fit, M is the number of fit parameters and i is the summation index. Also ψ_i^{exp} , Δ_i^{exp} and ψ_i^{mod} , Δ_i^{mod} are the experimental and modeled values of ψ and Δ , respectively. $\sigma_{\psi,i}^{\text{exp}}$ and $\sigma_{\Delta,i}^{\text{exp}}$ are the experimental standard deviations in ψ and Δ respectively, which were calculated from the known error bars on the calibration parameters and the fluctuation of the measured data over averaged cycle of the rotating polarizer and analyzer. Eq. (3) has the $2N$ and M in prefactor because there are two measured values included in the calculation for each ψ and Δ pair. The spectral dependencies of ψ and Δ determined for the as deposited and γ –irradiated at exposure doses of 100, 300 and 500 kGy of ZnO films on glass substrate are depicted in Fig. 5. Fig. 6 shows a good agreement between the measured ψ and Δ data (symbols) and the model fit (line) in the entirely measured wavelength range for as deposited and γ –irradiated at exposure doses of 100, 300 and 500 kGy of ZnO films on glass substrate. The estimated thicknesses for the surface roughness layer are 6.1, 5.8, 5.1 and 4. and the thicknesses for the ZnO dense layer are 233, 233, 234 and 232 nm. The fitted optical constants,

i.e. the refractive indices and extinction coefficients of as deposited and γ - irradiated at exposure doses of 100, 300 and 500 kGy of ZnO films on glass substrate are presented in Fig. 7 and Fig. 8, respectively. It is clearly observed that the refractive index of the investigated films increases with increasing the doses of γ -radiation. This result may be attributed to the increase in the density occurred in the investigated films with increasing irradiation doses. Two factors affecting the increasing of the density with irradiation doses, the first is displacement effect and the second is self-assembly behavior [17]. Fig. 8 shows that extinction coefficient decreases with decrease in photon energy, with sharp decrease near the band edge in the visible region. The absorption coefficient $\alpha(h\nu)$ of ZnO thin films can be calculated from the values of extinction coefficient k and λ using the known formula $k = \alpha\lambda/4\pi$. Fig. 9 shows the variation of the absorption coefficient, α against incident photon energy ($h\nu$) for the as-deposited and γ -irradiated nanocrystalline ZnO thin films. It is obviously shown that in the absorption edge region, the absorption coefficient slightly increases with the increase of

the doses of γ -radiation. Consequently, the values of the absorption coefficient in the absorption edge region of the investigated nanocrystalline ZnO films could be considered as a control parameter for which the nanocrystalline ZnO can be used as a radiation detector material. In addition, Fig. 9 shows that the absorption edge shifts toward the lower energy region with increasing the doses of γ - radiation. It is known, that in the vicinity of the fundamental absorption edge, for allowed direct band-to-band transitions, the absorption coefficient is described by:

$$\alpha(h\nu) = \frac{K (h\nu - E_g^{opt})^m}{h\nu} \quad (5)$$

where K is a characteristic parameter (independent of photon energy) for respective transitions, $h\nu$ denotes photon energy, E_g^{opt} is optical energy gap and m is a number which characterizes the transition process. Different authors [18-20] have suggested different values of m for different glasses, $m=2$ for most amorphous semiconductors (indirect transition) and $m = 1/2$ for most of crystalline semiconductor (direct transition). In few reports, the band gap of ZnO is classified as a direct

transition [21, 22]. Therefore, the allowed direct optical band gaps of ZnO films were evaluated from $(ah\nu)^2$ vs. $h\nu$ plots. Fig. 10 shows $(ah\nu)^2$ vs. $h\nu$ plots of as deposited and γ – irradiated at exposure doses of 100, 300 and 500 kGy of ZnO films. The tangential extrapolation to X-axis (energy) gives the band gap energy of direct transition. The values of direct E_g^{opt} are found to decrease in range extended from 3.27 to 3.32 with increasing γ –irradiation doses. The decrease of E_g^{opt} for direct transition may be attributing to the increase in crystallites size.

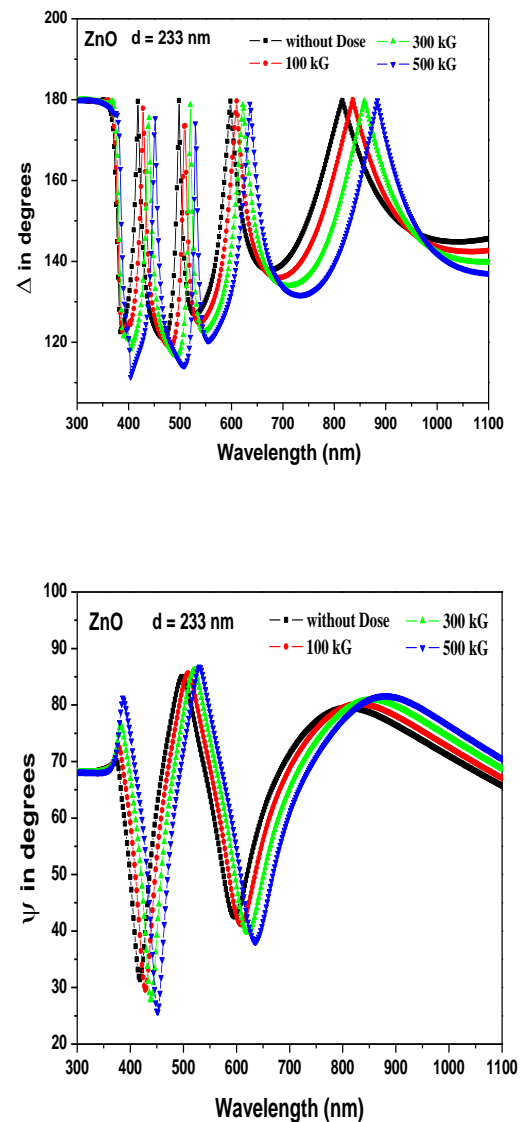


Fig. 5: Spectral ellipsometric data ψ and Δ of as-deposited and γ –irradiated doses of ZnO films grown on glass substrate.

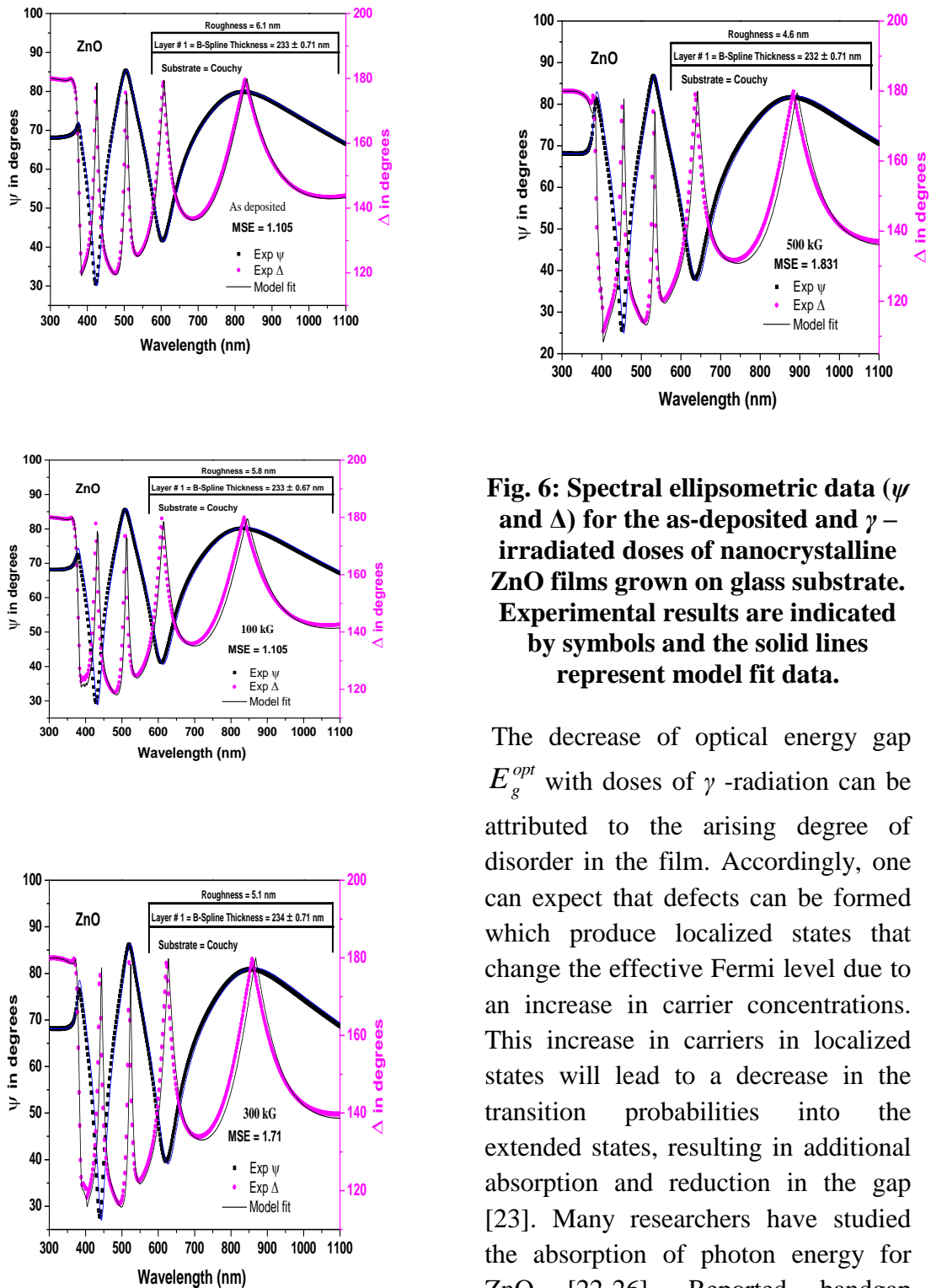


Fig. 6: Spectral ellipsometric data (ψ and Δ) for the as-deposited and γ -irradiated doses of nanocrystalline ZnO films grown on glass substrate. Experimental results are indicated by symbols and the solid lines represent model fit data.

The decrease of optical energy gap E_g^{opt} with doses of γ -radiation can be attributed to the arising degree of disorder in the film. Accordingly, one can expect that defects can be formed which produce localized states that change the effective Fermi level due to an increase in carrier concentrations. This increase in carriers in localized states will lead to a decrease in the transition probabilities into the extended states, resulting in additional absorption and reduction in the gap [23]. Many researchers have studied the absorption of photon energy for ZnO [22-26]. Reported bandgap energy value for the ZnO for as deposited is in the range of 3.21 to 3.3 eV, which is in good agreement with our report.

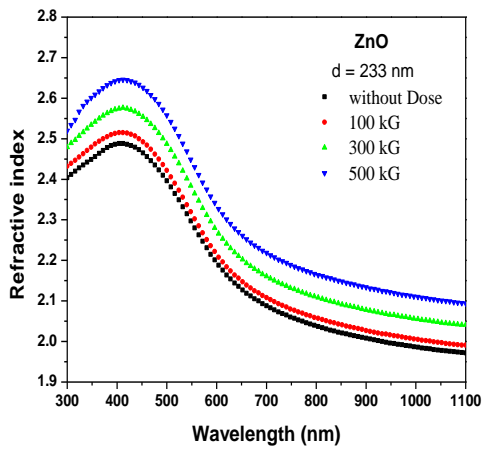


Fig. 7: The spectral dependence of refractive index n for the as-deposited and γ -irradiated doses of ZnO films.

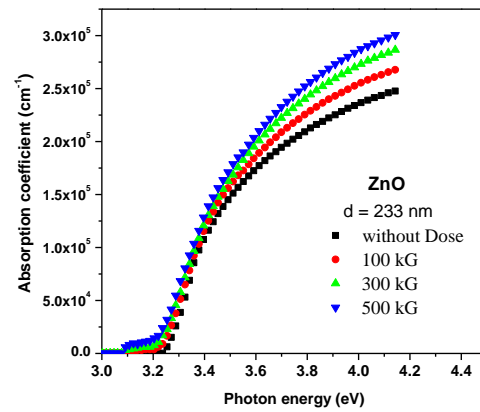


Fig. 9: The variation of the absorption coefficient, α against incident photon energy ($h\nu$) for the as-deposited and γ -irradiated doses of nanocrystalline ZnO thin films.

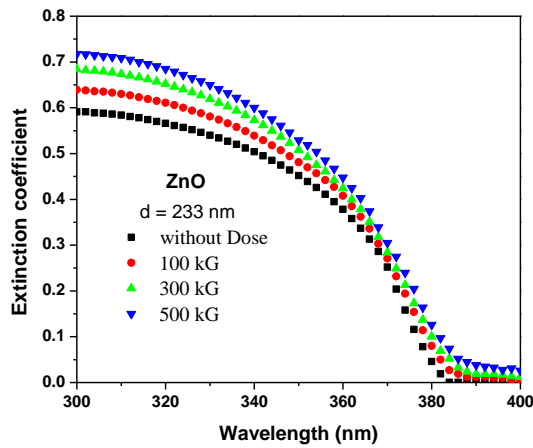


Fig. 8: The spectral dependence of extinction coefficient k of ZnO films of as-deposited and γ -irradiated doses.

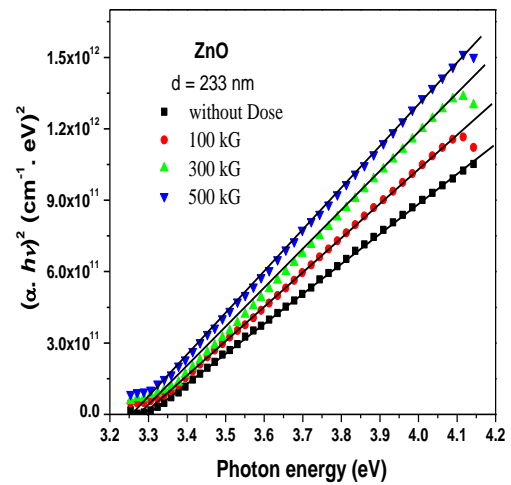


Fig. 10: Variation of $(\alpha h\nu)^2$ vs. $(h\nu)$ for the as-deposited and γ -irradiated doses of ZnO films.

4- Conclusions

A fine ZnO nanoparticles were prepared by a homogeneous precipitation method with an aqueous solution of zinc nitrate [$\text{Zn}(\text{NO}_3)_2 \cdot 6\text{H}_2\text{O}$] and citric acid [$\text{C}_6\text{H}_8\text{O}_7 \cdot \text{H}_2\text{O}$]. Thermo gravimetric (TGA) analysis and differential scanning calorimeter (DSC) were used to identify the calcinations temperature for obtaining a high purity of ZnO powder. Both crystallites size and microstrain ZnO of as deposited and γ -irradiated at exposure doses of 100, 300 and 500 kGy films were determined. It is observed that the crystallite size increases with increasing the doses of γ -radiation but the microstrain decreases. The increasing of the (D_v) may be attributed to the thermal effect during irradiation, which increases the crystallinity of film. But the decrease in (e) may be attributed to the reduction of lattice imperfections among the grain boundary due to the thermal effect during irradiation. The SE parameters (ψ and Δ) for ZnO films of as deposited and γ -irradiated at exposure doses of 100, 300 and 500 kGy were measured in the wavelength range 300–1100 nm and the optical constants, n and k of the ZnO films were determined by fitting the model function to the measured data using J.A. Woollam Corporation developed WVASE32 program. It is clearly observed that the refractive index of the investigated films increases with increasing the doses of γ -radiation. This result may be attributed to the increase in the density occurred in the

investigated films with increasing irradiation doses. The allowed direct band gaps of ZnO films were evaluated from $(ah\nu)^2$ vs. $h\nu$. The decrease of optical energy gap E_g^{opt} with doses of γ -radiation can be attributed to the arising degree of disorder in the film. Accordingly, one can expect that defects can be formed which produce localized states that change the effective Fermi level due to an increase in carrier concentrations.

Acknowledgment

The authors are grateful to Al Azhar university- Faculty of Science Physics department Assuit branch, for financial support. The authors thank professor A. El-Taher at College of Science, Qassim University, Saudi Arabia for measuring the samples and his valuables discussion during preparing the paper.

References

- [1] S.Y. Kuo, W.C. Chen, ChengF C. Superlattices Microstruct, 39,162 (2006).
- [2] H.M. Zhou, D.Q. Yi, Z.M. Yu, L.R. Xiao, J. Li, Thin Solid Films, 515,6909 (2007).
- [3] G. Srinivasan, R.T. Rajendra Kumar, J. Kumar, Opt. Mater, 30, 314 (2007).

- [4] E.J.L. Arredondo, A. Maldonado, R. Asomoza, D.R. Acosta, M.A.M. Lira, M. de la, L.Olvera, *Thin Solid Films*, 490,132 (2005).
- [5] V. Fathollahi, M.M. Amini, *Mater. Lett*, 50, 235 (2001).
- [6] T. Schuler, M.A. Aegerter, *Thin Solid Films*, 351,125 (1999).
- [7] H. Bahadur, S.B. Samanta, A.K. Srivastava, K.N. Sood, R. Kishore, R.K. Sharma, A. Basu Rashmi, M. Kar, P. Pal, V. Bhatt, ChandraF S., *J. Mater. Sci*,41,7562 (2006) .
- [8] H. Bahadur, A.K. Srivastava, R.K. Sharma, S. Chandra, *Nanoscale Res. Lett*,2, 4695 (2007).
- [9] H. Li, J. Wang, H. Liu, C. Yang, H. Xu, X. Li, H. Cui, *Vacuum*,77,57-62 (2004).
- [10] S.B. Majumder, M. Jain, P.S. Dobal, R.S. Katiyar, *Mater. Sci. Eng. B*,103, 16(2003).
- [11] B.D. Cullity, *The Elements of X-Ray Diffraction*, Addison–Wesley, Reading, MA, 1978, p. 102.
- [12] U. Pal, J.G. Serrano, P. Santiago, G. Xiong, K.B. Ucer, R.T. Williams, *Opt. Mater*,29,65(2006).
- [13] E. R. Shaaban, Ishu Kansal and José M. F. Ferreira thicknesses *Physica B: Condensed matter*,404, 3571 (2009)
- [14] E. R. Shaaban, N. Afify, A. El-Taher, *J.AlloysCompd*, 482, 400 (2009).
- [15] S. K.Biswas, S. Chaudhuri and A. Choudhury, *Phys. Status. Solidi (a)*, 105, 467 (1988).
- [16] H. Fujiwara, *i. S. Ellipsometry: and Principles and Applications*, Wiley, West Sussex, UK, (2007).
- [17] J.W. Park, K.N. Choi, S.H. Baek , K.S. Chung and H. Lee, 52,1868 (2008).
- [18] J.H. Bhang, M. Lee, H.L. Park, I.W. Kim, J.H. Jeong and K.J. Kim, *Appl. Phys. Lett*, 79, 1664 (2001).
- [19] E.A. Davis and N.F. Mott, *Philos. Mag*, 22, 903 (1970).
- [20] E.R. Shaaban, *Philos. Mag*, 88, 781 (2008).
- [21] N. Khemiri, B. Khalfallah, D. Abdelkader and M. Kanzari, *International Journal of Thin Films Science and Technology*, 3, 7 (2014).
- [22] T. Makino, C.H. Chi a, T.T. Nguen, Y. Segawa, *Appl. Phys. Lett*, 77, 1632 (2000).
- [24] Liua Y.C., Tunga S.K., Hsieh J.H. *Journal of Crystal Growth* ,287,105 (2006).
- [25] Chen K.J., Fang T.H, Hung F.Y., Ji L.W. , Chang S.J., Young S.J., Hsiao Y.J. *Applied Surface Science*, 254,5791 (2008).
- [26] Wasan R. Saleh, Nada Saeed M., Wesam A. Twej, Mohammed Alwan *Advances in Materials Physics and Chemistry*, 2, 11 (2012).